

# Studying sequences of resonant orbits to perform successive close approaches with the Moon

Jorge Kennety S. Formiga · Antonio F. B. A. Prado

Received: 17 June 2013 / Accepted: 23 September 2014 / Published online: 17 October 2014  
© The Brazilian Society of Mechanical Sciences and Engineering 2014

**Abstract** This research shows a study of the dynamical behavior of a spacecraft that performs a series of close approaches with the Moon. This maneuver is also known in the literature as Gravity-Assisted Maneuver. It is a technique to reduce the fuel expenditure in interplanetary missions by replacing maneuvers based on engines by passages near a massive body. The spacecraft moves under the gravitational attraction of the two bodies that dominate the system, the Earth and the Moon in the present study, and has a negligible mass. The main assumption to study this problem is that the motions are planar everywhere. In particular, we are looking for geometries that allow multiple close approaches without any major correction maneuvers. It means that the only maneuvers allowed are the negligible ones made to force the spacecraft to pass by the Moon with a specified distance from its surface. So, resonant orbits are required to obtain the series of close approaches. Analytical equations are derived to obtain the values of the parameters required to get this sequence of close approaches. The main motivation for this study is the existence of several studies for missions that has the goal of studying the space around the Earth–Moon system using multiple close approaches to make the spacecraft to cover a larger portion of the space

without any major maneuver. After obtaining the trajectories, the criterion of Tisserand is used to validate the trajectories found. Then, a verification of the accuracy of the “patched-conics” method for the Earth–Moon system is made.

**Keywords** Astrodynamics · Orbital maneuvers · Close approach maneuvers · Space trajectories

## 1 Introduction

In aerospace engineering, depending on the purpose of the mission, the trajectory of the spacecraft can be controlled by several physical forces. In the present research, the focus is on missions that use the close approach maneuver to act in part of the trajectory. It is well known that, when a close approach occurs in the neighborhood of a massive body (a planet or a natural satellite), the spacecraft experiences physical forces which depend on the relative velocity between the spacecraft and the planet and also on the distance separating the two of them at the point of the closest approach.

This idea appeared in the space program to find alternatives to reduce the fuel expenditure in interplanetary missions. The standard approaches to solve problems related to orbital maneuvers, without the use of close approaches, assume that the spacecraft has an engine that can deliver a force to the spacecraft to control its motion. This force may have a low magnitude that is applied during a finite time or a high magnitude that is applied during a negligible time. The first option is called “continuous thrust approach” and references [4, 14, 20–22, 40] show some details on that approach. The second alternative uses the idea of an impulsive thrust, where the force is assumed to have an infinity

---

Technical Editor: Fernando Alves Rochinha.

---

J. K. S. Formiga · A. F. B. A. Prado (✉)  
National Institute for Space Research - INPE, Av dos Astronautas  
1758, São José dos Campos, SP, Brazil  
e-mail: bertachiniprado@bol.com.br

J. K. S. Formiga  
e-mail: jkennety@yahoo.com.br

J. K. S. Formiga  
College of Technology, FATEC-SJC, São José dos Campos, SP,  
Brazil

magnitude. This is very popular in the literature and many references used this approach, starting with [17]. Some other examples are [13, 15, 16, 19, 31, 35–38].

Looking again in the literature, searching for researches considering close approaches as an alternative for orbital maneuvers, there are several studies and missions using this technique, including researches as early as Ref. [18], from 1961. From several missions, we can mention an important example, occurred in December 1973, with the encounter of the Pioneer 10 with the planet Jupiter. The description of this encounter is shown in the detailed ephemerides prepared by NASA's Jet Propulsion Laboratory and Ames Research Center [1]. Ref. [2] also shows several aspects of this maneuver, as well as Ref. [3]. There are also several other studies that can be mentioned, like the study of transfer orbits to find trajectories linking the Lagrangian points and the primaries of the system [28, 30]. In terms of practical missions that use this technique, it is possible to mention [5–10, 23, 39, 41, 43] which show several applications of the close approach in orbital maneuvers. Some other studies considered variations of this problem, like the combination of impulsive or low thrust maneuvers during the close approach [26, 27, 32], the existence of an atmosphere during the swing-by [29], noncircular orbits for the primaries [33] or a three-dimensional swing-by [11].

The focus of the present paper is to find a series of close approaches with the Moon, which can be used to analyze possible missions to cover the space around the Earth–Moon system. It means that it is desired to make the spacecraft to have different values of apogees, to study larger areas of the space without the need of fuel consumption. The orbital elements, energy, angular momentum and velocity of the spacecraft with respect to the Earth are changed by each of these close approaches. The dynamical system given by the “patched conics” is used and the motion is assumed to be planar everywhere. A series of two-body problems are considered to generate analytical equations that describe the problem. The orbital elements of the spacecraft before and after this close encounter are calculated to detect the changes in the trajectories. The goal is to study the orbital characteristics (orbital elements, velocity, energy and angular momentum) after each close approach to know how this trajectory will evolve, to have a better understanding of the possible applications. A study with similar ideas was made by Strange and Longuski [23, 25], where a graphical approach based on the criterion of Tisserand [24, 42] was developed to evaluate the potential of multiple swing-bys passing by different bodies of the Solar System. This research evaluates the swing-bys assuming that the celestial bodies are always in the correct position for the close approach, which is an excellent idea to evaluate the possibilities of the maneuvers. The present paper adds the concern of finding resonant orbits for

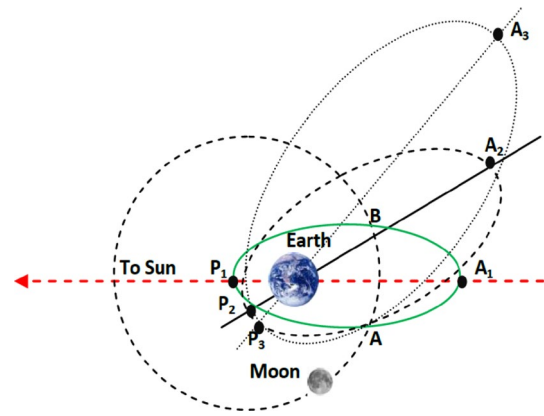


**Fig. 1** Overview of the orbital characteristics for some swing-bys

the sequence of trajectories, so making sure that the proper positions occur and the sequence of swing-bys found is real and not only potential.

The main motivation for this research is based on some applications of close approaches that have the goal of keeping a spacecraft around the Earth, but making several passages by the Moon to allow the spacecraft to pass by different parts of the space near this system. This strategy has the goal of studying larger areas of the space without making orbital maneuvers that require fuel consumption. The gravity of the Moon supplies the spacecraft with the energy required to change the location of the apogee of the orbit, making the spacecraft to cover a larger area of the space. This is an interesting problem, because there is a conflict of objectives. It is necessary to reach larger variations of energy, but those changes cannot be large enough to cause an earlier escape of the spacecraft from the Earth. One solution is to find a series of values for the closest approach distance for each passage by the Moon (assumed to be the only control variable), such that it generates a series of orbits that, by making successive variations in the energy of the spacecraft, keep it passing by different positions in space. Those variations need to be calculated in such a way that the orbits are all resonant with respect to the Moon, so a new close encounter will occur between the spacecraft and the Moon after a given time without the need of maneuvers based on fuel consumption. In the present paper, analytical equations are derived to solve this problem. Some references showing this type of application are [12, 23]. A geometric representation can be seen in Fig. 1, where the spacecraft is in orbit around the Earth and performing multiple close approaches with the Moon. It is shown that the apogee of the trajectory of the spacecraft around the Earth is changing, passing by the points  $A_1$ ,  $A_2$  and  $A_3$ . Figure 1 shows the first three passages of a series that can be much longer. The perigee distance also changes, giving even more possibilities to study different areas of the space near the Earth.

Looking at those missions, some interesting questions appear: how many times can the spacecraft makes close approaches with the Moon before you have a passage that makes its orbit to become hyperbolic and then escape from the system? Also, during this process, which values of semi-major axis and eccentricities can be covered? Which of those trajectories can be used in practical applications, considering that the perigee of the orbit has to be above the surface of the Earth and that the closest distance during the passage by the Moon has to be above the lunar surface? So, in the present paper, a study of those questions is made. The intermediate orbits are also studied in some detail.

A more detailed analysis comparing the “patched-conics” approach with the restricted three-body problem is made for the Earth–Moon system, with the goal of estimating the errors of the model and also showing the regions where the approximation is better.

## 2 Mathematical model

It is well known that the “patched-conics” approximation offers an efficient procedure to study interplanetary trajectories. By partitioning the overall trajectory in a series of two-body problems, it is possible to greatly simplify the mission analysis. The basic assumption of the “patched-conics” approximation is that the trajectory of a spacecraft is determined by the gravitational field of the body that dominates the motion of the spacecraft in all phases of the mission. It also assumes that the dynamical system is dominated by two main bodies that are in circular orbits around their center of mass and the spacecraft is moving under the gravitational attraction of those two primaries. So, in this approach, this problem can be studied assuming a system formed by three bodies: The Earth, as the main massive primary ( $M_1$ ), the Moon, as a secondary mass ( $M_2$ ) that is orbiting  $M_1$ , and a spacecraft with infinitesimal mass ( $M_3$ ) that remains orbiting the primary and makes a close approach with  $M_2$ . This close approach has the same effect of applying a single impulse with zero cost to modify the orbit of the spacecraft. Figure 2 explains the geometry involved in this close approach with the Moon. The spacecraft is initially in orbit around the Earth, cross the sphere of influence of the Moon and then it goes back to another orbit around the Earth. Point  $P_1$  represents the beginning of the approach and point  $P_2$  represents the end of the close approach in Fig. 2. In the real motion, there is no exact point where the spacecraft changes its orbit from around the Earth to around the Moon, but both bodies are acting all the time. The correct model to study this problem is the Restricted Three-Body Problem, but it does not allow closed form solutions. It means that there is a large zone where both bodies are acting at the same time. To simplify

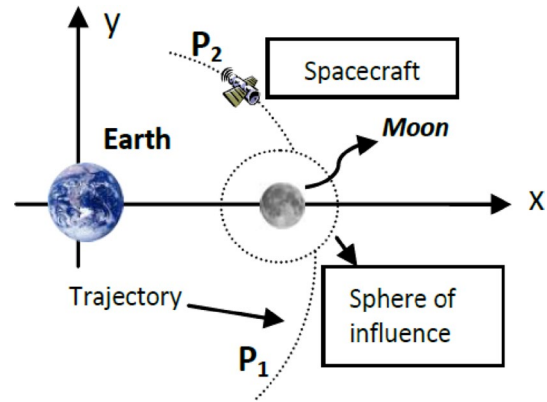


Fig. 2 A close approach between a spacecraft and the Moon

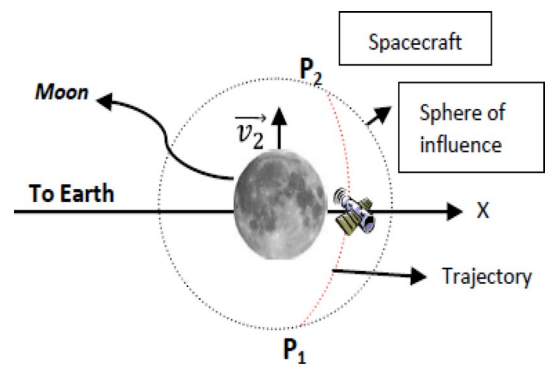


Fig. 3 Detailed view of the close approach between a spacecraft and the Moon

the analytical study, it is assumed that the point where the spacecraft reaches the Moon is at the Earth–Moon distance, which means that the Moon’s sphere of influence is neglected. A better model would choose a point somewhere between the sphere of influence and the surface of the Moon, much closer to the surface of the Moon. Using the two-body approximation it is not possible to determine this point. The accuracy of the present approximation is studied later in the present paper and it shows that it does not give results too far from the real ones.

An amplification of Fig. 2 can be seen in Fig. 3, which shows in more detail when the spacecraft crosses the sphere of influence of the Moon in a hyperbolic trajectory with respect to the Moon.

Figure 4 shows some of the variables that are used to identify one close approach trajectory:  $r_{ap}$  (the distance from the spacecraft to the center of  $M_2$  (the Moon) at the moment of the closest approach),  $\vec{v}_{\infty}^-$  and  $\vec{v}_{\infty}^+$  (velocity of  $M_3$  with respect to  $M_2$ , before and after the swing-by, in the inertial frame),  $\vec{v}_2$  (velocity of  $M_2$  with respect to  $M_1$ ),  $\delta$  (half of the angle of the curvature due to the close approach) and  $\psi$  (angle of approach).

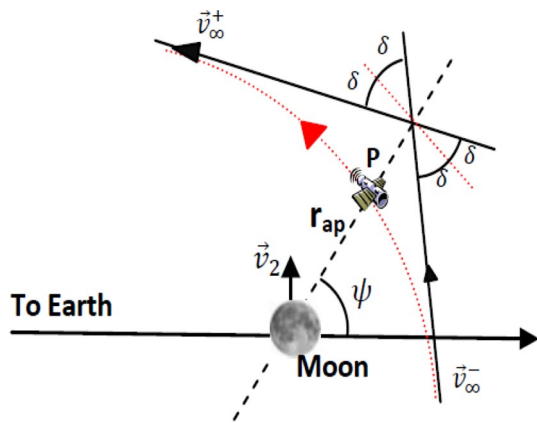


Fig. 4 Variables of the close approach

The velocity and orbital elements of the spacecraft are changed by the close approach with the Moon. The orbital elements ( $a$  = semi-major axis,  $e$  = eccentricity), energy ( $E$ ) and angular momentum ( $C$ ) of the spacecraft before the encounter with the Moon are obtained from the equations:

$$a = \frac{r_a + r_p}{2} \tag{1}$$

$$e = 1 - \frac{r_p}{a} \tag{2}$$

$$E = -\frac{\mu}{2a} \tag{3}$$

$$C = \sqrt{\mu a(1 - e^2)} \tag{4}$$

where  $r_p$  is the perigee of the orbit of the spacecraft around the Earth,  $r_a$  is the apogee of the orbit of the spacecraft around the Earth and  $\mu$  is the gravitational parameter of the Earth =  $3.98600 \times 10^5 \text{ km}^3/\text{s}^2$ . To determine the velocity of the spacecraft with respect to the Moon in the moment that the close approach occurs, it is necessary to obtain the magnitude of the velocity of the spacecraft with respect to the Earth in that moment ( $v_i$ ), as well as the true anomaly of the spacecraft at this point. It is possible to do that using the following equations, all of them obtained using the above explained approximation of neglecting the sphere of influence of the Moon in the geometry of the encounter:

$$|\vec{v}_i| = \sqrt{\mu \left( \frac{2}{r_{EM}} - \frac{1}{a} \right)} \tag{5}$$

$$\theta = \cos^{-1} \left[ \frac{1}{e} \left( \frac{a(1 - e^2)}{r_{EM}} - 1 \right) \right] \tag{6}$$

where  $r_{EM}$  is the distance between the Earth and the Moon. Equation (6) has two solutions ( $\theta_A$  and  $\theta_B$ ), that corresponds

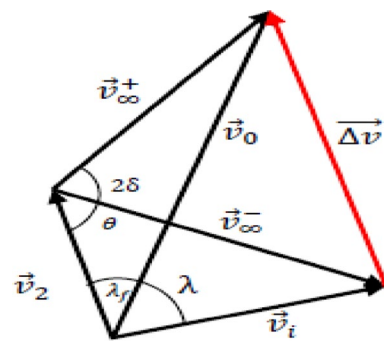


Fig. 5 Vectorial sum that explains the swing-by

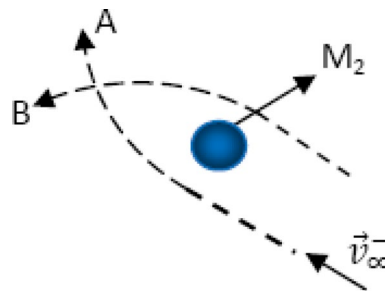


Fig. 6 Possible rotations of the velocity vector

to the points A and B, respectively, as shown in Fig. 1. In this study, we will consider the solution given by the angle  $\theta_A$ , which means that the spacecraft reaches the Moon's orbit before it reaches the apogee of its orbit, considering a counterclockwise geocentric trajectory. The solution  $\theta_B$  is not considered, because there is a symmetry in the system and the results are similar to the ones obtained by the solution for  $\theta_A$ . From these values it is possible to calculate the angle  $\gamma$  between the inertial velocity of the spacecraft and the velocity of the body  $M_2$ :

$$\gamma = \tan^{-1} \left[ \left( \frac{e \sin \theta}{1 + e \cos \theta} \right) \right] \tag{7}$$

Therefore, the magnitude of the velocity of the spacecraft with respect to the Moon, in the moment that the approach starts ( $v_\infty$ ), will be determined by:

$$v_\infty = \sqrt{v_i^2 + v_2^2 - 2v_i v_2 \cos \gamma} \tag{8}$$

when  $\vec{v}_2$  is the velocity of  $M_2$  with respect to  $M_1$  and  $\vec{v}_i$  and  $\vec{v}_0$  are the velocities of  $M_3$  with respect to  $M_1$ , before and after the swing-by, respectively, in the inertial frame. This can be seen in Fig. 5, which shows how to obtain the  $\Delta \vec{v}$  generated by the close approach. In Fig. 5,  $\lambda$  represents the angle between  $\vec{v}_i$  and  $\vec{v}_0$ ,  $\lambda_f$  represents the angle between  $\vec{v}_2$  and  $\vec{v}_0$  and  $\theta$  represents the angle between  $\vec{v}_2$  and  $\vec{v}_\infty^-$ . There are two possibilities for the spacecraft when passing by the Moon

(Fig. 6): the one assuming that the rotation of the velocity vector is in the counterclockwise sense (using point B of Fig. 6, giving the angle  $\psi_1$ ) and the one assuming that this rotation is in the clockwise sense (using point A of Fig. 6, giving the angle  $\psi_2$ ). These two values are obtained from:

$$\psi_1 = \pi + \beta + \delta \tag{9}$$

$$\psi_2 = 2\pi + \beta - \delta$$

where

$$\beta = \cos^{-1} \left[ -\frac{v_i^2 - v_2^2 - v_\infty^{-2}}{2v_2v_\infty} \right] \tag{10}$$

$$\delta = \sin^{-1} \left[ \frac{1}{1 + \frac{r_{ap}v_\infty^2}{\mu}} \right] \tag{11}$$

$\mu$  is the gravitational parameter of the Moon. In this moment it is possible to obtain the variations of the two-body energy and angular momentum in the system formed by the spacecraft and the Earth, from the equations [3]:

$$\Delta v = |\vec{v}_0| - |\vec{v}_1| = 2|\vec{v}_\infty| \sin \delta \tag{12}$$

$$\Delta E = E_+ - E_- = -2v_2v_\infty \sin \delta \sin \psi \tag{13}$$

$$\Delta C = \frac{\Delta E}{\omega} \tag{14}$$

where  $\omega$  is the angular velocity of the motion of the primaries,  $\delta$  is half of the angle of deflection due to the close approach and  $E_-$ ,  $E_+$  are the energy before and after the swing-by, respectively. Finally, having determined the variation of energy and angular momentum after the swing-by, it is possible to obtain the semi-major axis and the eccentricity after the close approach using the equations:

$$a = -\frac{\mu}{2E} \tag{15}$$

$$e = \sqrt{1 - \frac{C^2}{\mu a}} \tag{16}$$

$$\cos(\delta) = \left\{ \frac{1}{2} \sqrt{3 + \text{Cos}(2\beta) - D} \right\}$$

$$D = \frac{2(v_2v_\infty \Delta E \text{Cos}(\beta) + \sqrt{\Delta E [v_2v_\infty \sin(\beta)]^2 [2v_2v_\infty \text{Cos}(\beta) - \Delta E] + [v_2v_\infty \sin(\beta)]^4})}{(v_2v_\infty)^2} \tag{23}$$

The next important step is to find the value of the distance that the spacecraft has to pass from the Moon ( $r_{ap}$ ) to achieve an orbit that has a larger value for the apogee (so, achieving the goal of making the spacecraft to pass by different positions in space), but also sending the

spacecraft to an orbit that is resonant with the orbit of the Moon, such that a new encounter will occur between the spacecraft and the Moon, allowing a new swing-by. The approach used here to solve this question is to make a list of resonant orbits and then calculating the energy of each orbit. After that, this list is organized in the order of increasing values of energy. Based on that list, a search is made to find the value of  $r_{ap}$  for each passage that makes the orbits of the spacecraft to follow the desired sequence.

The first task is to obtain an equation that gives  $r_{ap}$  as a function of the variation in the energy desired. To complete this goal, it is necessary to calculate the value of  $\delta$  ( $0 \leq \delta \leq 90$ ), half of the angle of deflection, due to the close approach. Considering Eq. (13) for the variation of energy:

$$\Delta E = -2v_2v_\infty \sin \delta \sin \psi_2 \tag{17}$$

where, from Eq. (9), we have  $\psi_2$ .

Then

$$\Delta E = -2v_2v_\infty \sin \delta \sin [2\pi + \beta - \delta] \tag{18}$$

Through a trigonometric expansion, it is possible to get:

$$\Delta E = -2v_2v_\infty \sin(\delta) [\sin(2\pi + \beta) \cos(\delta) - \cos(2\pi + \beta) \sin(\delta)] \tag{19}$$

Considering now that  $\sin(2\delta) = 2 \sin(\delta) \cos(\delta)$ , and defining the constants

$$A = \frac{\sin(2\pi + \beta)}{2}; \quad B = \cos(2\pi + \beta);$$

$$C = -\frac{\Delta E}{2v_2v_\infty} \tag{20}$$

we have:

$$A \sin(2\delta) - B \sin^2(\delta) = C \tag{21}$$

Then the analytical solution is:

$$\delta = \text{ArcCos} \left[ \frac{1}{\sqrt{2}} \sqrt{\frac{A^2 + 2B(B+C) - A\sqrt{A^2 - 4C(B+C)}}{A^2 + B^2}} \right] \tag{22}$$

or, by simplification,

The distance of close approach is obtained by reorganizing Eq. (11) to give:

$$r_{ap} = \frac{\mu}{v_\infty^2} \left[ \frac{1}{\sin(\delta)} - 1 \right] \tag{24}$$

where  $0 \leq \delta \leq 90$ .

A similar study can be made for the case where the angle of approach is  $\psi_1 = \pi + \beta + \delta$ . The final result is the same. This fact is expected, because a specific value for the variation in energy is required, there is only one solution for the problem.

### 3 Tisserand's Criterion

The Tisserand's criterion is an important method that can be used in the study of gravity-assisted maneuvers. It was presented by the French astronomer Francois Felix Tisserand and can be obtained from the Jacobian constant by making the approximation of neglecting the mass of the secondary primary. A detailed explanation of this derivation is available in Ref. [44], so the whole proof is not repeated here. It is an equation, developed in dimensionless coordinates, based on the circular-restricted three-body problem model. This method can be used to find sequences of orbits similarly to what is done here, but it does not give the parameters required to obtain the sequence, as done by the present methodology. But, besides those limitations, it is an important form to verify the results found in the present research, because it can validate the sequence of orbits. The method says that, for a spacecraft making a close approach with a celestial body, it has to nearly satisfy the equation [2, 6, 42]:

$$\frac{1}{a_i} + 2\sqrt{a_i(1 - e_i^2)} \cos i_i \approx \frac{1}{a_0} + 2\sqrt{a_0(1 - e_0^2)} \cos i_0 \quad (25)$$

The subscripts indicate that, before the swing-by, the spacecraft has orbital elements  $a_i$ ,  $e_i$  and  $i_i$  and, after the swing-by, it has orbital elements  $a_0$ ,  $e_0$  and  $i_0$ .

### 4 Numerical study

In this section, simulations are performed to analyze the orbital characteristics of a spacecraft that performs a series of close approaches with the Moon. It is assumed that the spacecraft starts its motion in a given orbit around the Earth. This orbit is specified by its perigee and apogee distances. The "patched-conics" model is used and the procedure studies successive close approaches. To limit the number of swing-bys, a maximum number of revolutions for the Moon between two successive close approaches are specified. Several simulations were made and the number of a maximum of five revolutions for the Moon between two close approaches was chosen. This number generates a large number of potential swing-bys. The term "potential swing-bys" is used because some of

the trajectories obtained may require a value smaller than the radius of the Moon for a periaapsis distance for one of the passages of the spacecraft by the Moon, or an orbit with perigee below the surface of the Earth. Those trajectories have to be excluded from the list of useful trajectories. A number higher than five would generate orbits with too large periods, which have little practical interest and that would be too much influenced by other perturbations. Those perturbations are not considered here, because the idea of the present paper is to study possible trajectories and not making final decisions on which orbit to use. This decision is left for a more detailed study of the trajectories, using better models for the dynamics. Table 1 shows the orbits, including the information of the number of periods of the Moon before the next close approach, the equivalent number of orbits of the spacecraft, the period (in days) of the orbit of the spacecraft, the respective semi-major axis (km), and the order of the resonance, that is the number of revolutions of the spacecraft followed by the number of revolutions of the Moon between two successive encounters.

Based on Table 1, it is possible to order these orbits to have increasing values of the energy and then search for values of  $r_{ap}$  for each passage that can make the spacecraft to follow this series. After that, the energy, angular momentum and orbital elements of the orbits are analyzed after each close approach, to show the histories of their evolution. The following assumptions are considered in those calculations:

- (1) The close approach will be at the point A (Fig. 1);
- (2) The Sun and the Earth (or any other perturbations) do not affect the motion of the spacecraft when it is close to the Moon;
- (3) The energy (E) and angular momentum (C) will be analyzed after and before the swing-bys.

During these calculations, it is necessary to take into account that some orbits require a value for the perigee below the surface of the Earth, which means that they are not practical. One of the advantages of this analytical approach is exactly to show this situation, so it is possible to see the first orbit of the sequence that does not have this problem. Table 2 shows, from the results obtained, those impossible orbits, with the orbits classified in the order of increasing energy. It has the number of the swing-bys, the orbital period (days), the distance of the closest approach obtained from the algorithm (in units of radius of the Moon), semi-major axis (km), eccentricity, energy ( $\text{km}^2/\text{s}^2$ ), perigee distance (km), apogee distance (km), half of the deflection angle (rad), angle of approach (rad), order of the resonance and the time elapsed since the start of the sequence of swing-bys (days). Orbit number 9 has a perigee

**Table 1** The resonant orbits for the spacecraft passing by the Moon

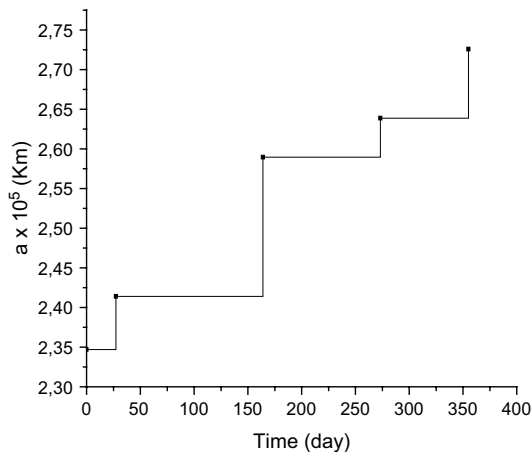
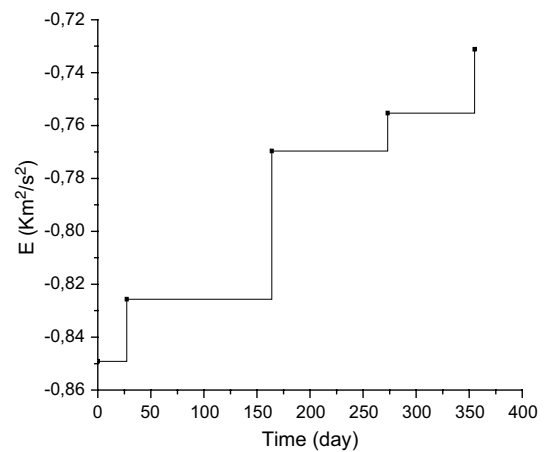
Number of revolutions of the Moon between two successive swing-bys	Number of revolutions of the spacecraft between two successive swing-bys	Period of the spacecraft (days)	Semi-major axis of the spacecraft (km)	Order of the resonance
1	1	27.3216	383,182	1:1
	2	13.6608	241,390	2:1
2	1	54.6432	608,264	1:2
	3	18.2144	292,423	3:2
	5	10.9286	208,023	5:2
3	1	81.9647	797,052	1:3
	2	40.9824	502,111	2:3
	4	20.4912	316,310	4:3
	5	16.3929	272,588	5:3
	7	11.7092	217,815	7:3
	8	10.2456	199,263	8:3
4	1	109.286	965,559	1:4
	3	36.4288	464,192	3:4
	5	21.8573	330,217	5:4
	7	15.6123	263,864	7:4
	9	12.1429	223,160	9:4
5	11	9.93512	195,217	11:4
	1	136.608	1120,430	1:5
	2	68.304	705,828	2:5
	3	45.536	538,648	3:5
	4	34.152	444,644	4:5
	6	22.768	339,327	6:5
	7	19.5154	306,187	7:5
	8	17.076	280,108	8:5
	9	15.1787	258,955	9:5
	11	12.4189	226,529	11:5
	12	11.384	213,762	12:5
	13	10.5083	202,655	13:5
	14	9.75771	192,886	14:5

**Table 2** Orbits with perigee too low to be used in the sequence of swing-bys

Swing-by	Orbital period (day)	$r_{ap}$ (radius of the Moon)	$a$ (km)	$e$	Energy	$r_p$ (km)	$r_a$ (km)	$\delta$ (°)	$\psi$ (°)	Resonance	Time (days)
0	13.097	–	234,698.97	0.9592	–0.8492	9,579.55	459,818.4	36.97	358.88	–	0
1	9.7577	16.50	192,885.78	0.9980	–1.0333	377.58	385,393.98	8.70	357.67	14:5	136.61
2	9.9351	9.61	195,216.77	0.9969	–1.0209	606.73	389,826.80	13.55	357.48	11:4	245.89
3	10.2456	6.76	199,262.89	0.9944	–1.0002	1,114.32	397,411.46	17.65	358.43	8:3	256.14
4	10.5083	5.19	202,654.70	0.9919	–0.9834	1,636.98	403,672.42	21.23	358.00	13:5	392.75
5	10.9286	4.03	208,023.42	0.9874	–0.9581	2,623.31	413,423.53	24.97	358.26	5:2	447.39
6	11.3840	3.37	213,762.45	0.9819	–0.9323	3,863.88	423,661.02	27.77	358.94	12:5	458.78
7	11.7092	2.93	217,814.97	0.9778	–0.9150	4,839.20	430,790.74	30.08	358.75	7:3	540.74
8	12.1429	2.61	223,160.45	0.9721	–0.8931	6,233.35	440,087.56	32.04	359.29	9:4	650.03
9	12.4189	2.14	226,528.98	0.9684	–0.8798	7,166.99	445,890.98	35.42	357.33	11:5	786.63

**Table 3** Sequence of orbits performing close approaches with the Moon

Swing-by	Orbital period (day)	$r_{ap}$ (radius of the Moon)	$a$ ( $10^3$ km)	$e$	Energy	$R_p$ ( $10^3$ km)	$R_a$ ( $10^3$ km)	$\delta$ ( $^\circ$ )	$\psi$ ( $^\circ$ )	Resonance	Time (days)	Tisserand's criterion
0	13.097	–	234.7	0.9592	–0.8492	9.56	459.82	36.97	358.88	–	0	1.0398
1	13.661	1.59	241.4	0.9516	–0.8256	11.68	471.1	40.55	357.54	2:1	27.32	1.0397
2	15.179	1.33	258.95	0.9321	–0.7696	17.58	500.32	43.60	359.41	9:5	163.93	1.0395
3	15.612	1.21	263.86	0.9269	–0.7553	19.30	508.43	45.17	359.03	7:4	273.22	1.0394
4	16.393	1.09	272.59	0.9179	–0.7311	22.39	522.78	46.91	359.23	5:3	355.18	1.0392
5	17.076	0.97	280.11	0.9105	–0.7115	25.08	535.13	48.81	358.86	8:5	491.79	1.0391
6	18.214	0.84	292.42	0.8991	–0.6815	29.51	555.33	51.08	358.88	3:2	546.43	1.0390

**Fig. 8** Semi-major axis of the spacecraft as a function of time**Fig. 7** Energy of the spacecraft as a function of time

above the surface of the Earth, but it is too close to the atmosphere (7,166.99 km from the center of the Earth), so it was also removed from this list of practical trajectories.

The remaining orbits are considered the possible ones for the sequence. They are shown in Table 3 and they represent the correct sequence of swing-bys, with respect to time, that keeps the spacecraft increasing energy, semi-major axis and apogee distance. Table 3 shows the same quantities as shown in Table 2. They are all obtained starting from a given initial orbit for the spacecraft around the Earth. The sequence of swing-bys presented corresponds to a single trajectory, so they all have similar values for the Tisserand's parameter. This is the meaning of this parameter. For a single trajectory it is nearly constant. The  $r_{ap}$ , distance of the closest approach between the spacecraft and the Moon, is the key factor for the sequence, because it is assumed to be the only variable available to control the motion of the spacecraft. The radius of the Moon is called  $R_m$ , and it is assumed to have the value 1,737 km. The perigee distance of the initial orbit around the Earth is chosen to be  $r_p = 9,579.55$  km and the respective apogee distance is  $r_a = 459,818.40$  km. This choice is a little

arbitrarily. It was made based on the principles that it is necessary to have an initial orbit with a perigee distance that can be easily obtained by standard rockets and an apogee distance that is just above the lunar orbit. Those principles generate orbits that can be reached without excessive fuel consumption. Some preliminary tests with similar values showed that this value has little influence in the results obtained, since, after the first encounter, the sequence of  $r_{ap}$  controls the motion of the spacecraft. In this way, there is no need to make too many simulations. Tests with higher differences were also made, and some interesting conclusions are shown in the next session. Now, it is necessary to study the second restriction and see if the values of  $r_{ap}$  required are possible to reach, which means that it has to be larger than the radius of the Moon. Table 3 shows that the swing-bys are possible until the number 4. Swing-By number 5 has a value of  $r_{ap} = 0.97$ , so a passage below the surface of the Moon would be required. In this way, Figs. 7, 8, 9, 10, 11, 12, 13, 14 show the results for the sequence of possible swing-bys that are the ones numbered from 1 to 4. The value of the criterion of Tisserand showed in the last column of Table 3 confirms that the method proposed here

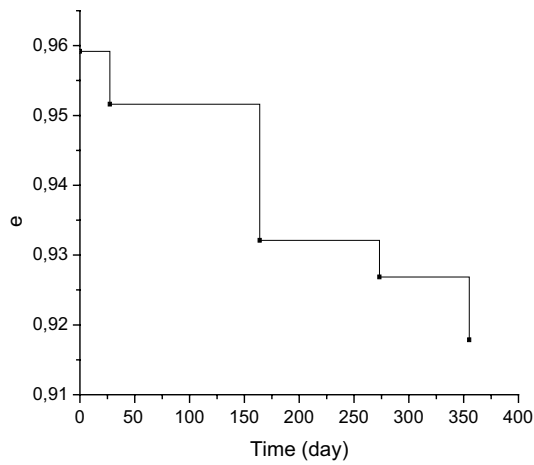


**Fig. 9** Eccentricity of the spacecraft as a function of time

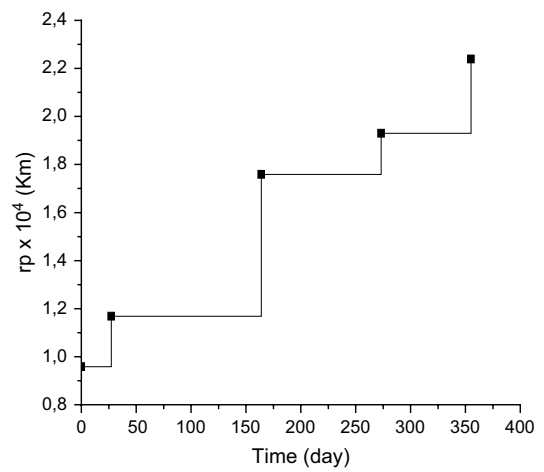


**Fig. 12** Perigee distance of the spacecraft as a function of time

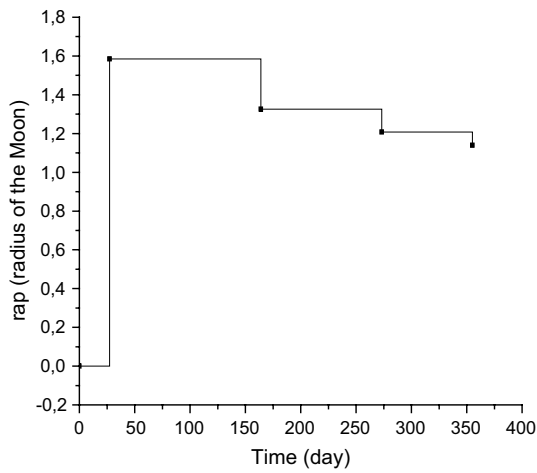


**Fig. 10**  $r_{ap}$  distance of the spacecraft as a function of time

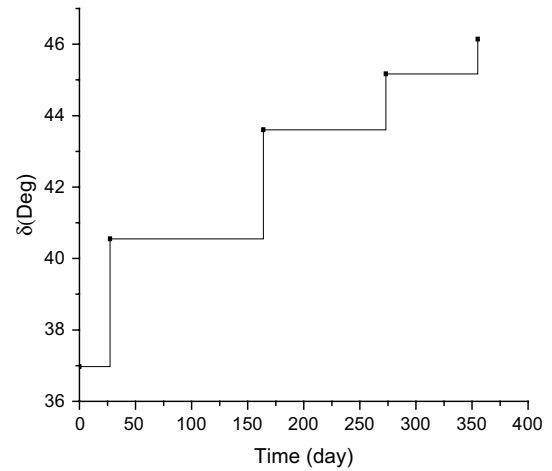


**Fig. 13** Half of the deflection angle as a function of time

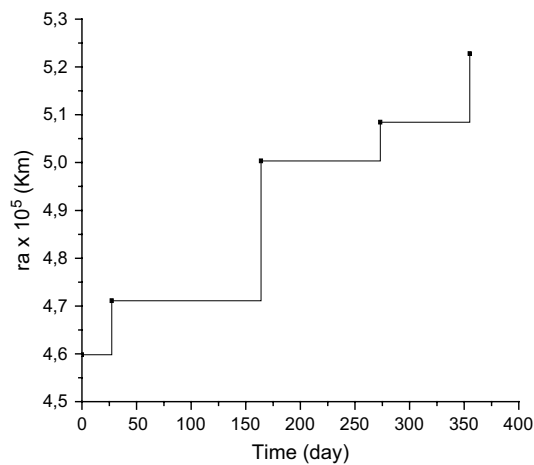


**Fig. 11** Apogee distance of the spacecraft as a function of time

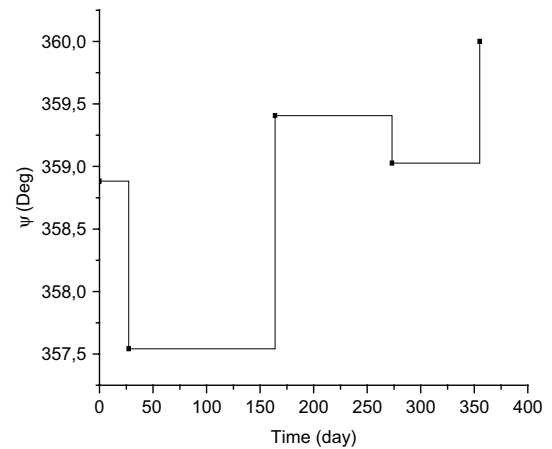


**Fig. 14** Angle of approach as a function of time

**Table 4** Sequence of orbits performing swing-bys with the Moon when  $r_p = 30,000$  km

Swing-by	Orbital period (day)	$r_{ap}$ (radius of the Moon)	$a$ ( $10^3$ km)	$e$	Energy	$r_p$ ( $10^3$ km)	$r_a$ ( $10^3$ km)	$\delta$ ( $^\circ$ )	$\psi$ ( $^\circ$ )	Resonance	Time (days)	Tisserand's criterion
0	13.96	–	244.91	0.8775	–0.814	30.00	459.82	40.35	360.61	–	0	1.1675
1	13.66	2.22	241.39	0.8834	–0.826	28.15	454.63	42.51	357.22	2:1	27.32	1.1675
2	15.18	1.95	258.96	0.8554	–0.770	37.45	480.46	45.96	359.33	9:5	163.93	1.1673
3	15.61	1.59	263.86	0.8482	–0.755	40.06	487.66	47.73	358.90	7:4	273.22	1.1672
4	16.39	1.43	272.59	0.8360	–0.731	44.7	500.47	49.69	359.14	5:3	355.18	1.1671
5	17.08	1.27	280.1	0.8262	–0.712	48.69	511.53	51.83	358.72	8:5	491.79	1.1670
6	18.21	1.11	292.42	0.8115	–0.682	55.12	529.72	54.38	358.73	3:2	546.43	1.1669
7	19.52	0.94	306.19	0.7970	–0.651	62.17	550.21	56.48	359.16	7:5	683.04	1.1667

found correct trajectories for the spacecraft, because the values are near constant, coherent with the level of approximation of the equations derived. The errors appear only in the fourth decimal digit.

Note that the spacecraft does not remain in every orbit the same amount of time. The times it stays in each orbit can be found in the plots, because the dots represent the instant of each swing-by. Those results show the expected evolution of the parameters and several interesting conclusions. The energy (see Fig. 7), and so the angular momentum (due to Eq. 14), the semi-major axis (see Fig. 8) and the apogee distance (see Fig. 11) increase after each swing-by. This characteristic is forced by the choice of the distance of the closest approach to the Moon, since the goal of the present research is to find this series. The energy goes from  $-0.8492 \text{ km}^2/\text{s}^2$  before the first passage to  $-0.7311 \text{ km}^2/\text{s}^2$  after the last possible swing-by, in increasing steps of smaller values, as shown in Fig. 7. This variation in energy causes the semi-major axis to go from 234,698.97 to 272,587.78 km (see Fig. 8), which corresponds to a variation of the apogee from 459,818.40 km (a little above the Lunar orbit) to 522,784.43 km, as shown in Fig. 11. The evolution of the perigee distance is shown in details in Fig. 12. It has larger increases, so making the spacecraft to pass by very different positions. The eccentricity shows a decreasing sequence of values, also divided in smaller steps, as can be seen in more details in Fig. 9. The time span for this sequence is 355.18 days, very close to 1 year. The values of  $r_{ap}$  have a very interesting behavior. It decreases from passage to passage. The reason for this fact is that it is necessary to compensate the increase of the velocity of the spacecraft. Equations (11) and (13) show that the variation of the energy depends on the velocity of approach and the periapsis distance of the close approach. The other parameters are all constants. So, since every passage increases the energy of the spacecraft and all passages have the same distance from the Earth (the Earth–Moon distance), the velocities of approach also increase from

passage to passage. It means that the periapsis distance has to decrease to be able to give the required variation in energy. This is shown in Fig. 10 and Table 3. In fact, this is the reason why the sequence of trajectories ends at a certain point before an escape occurs. There is a point (swing-by number 5), where a value below the lunar surface would be required to give the necessary increase in energy. Figure 13 shows the sequence of the angle of deflection, confirms these results, by showing that this quantity always increase to compensate the increase of the velocity of approach. Figure 14 complements this study, showing that the passages are always in front of the Moon, to increase the energy.

#### 4.1 Effects of the initial orbit

After studying the effects of the close approach distance, a study is made to verify the effects of the initial orbit of the spacecraft around the Earth in the sequence of close approaches. For values similar to the ones shown in the previous results, this change causes very little effects. The situation is a little bit different when the perigee is increased by larger values. The initial apogee distance is kept constant, because increasing this value had no effects in the results and reaching higher values would increase the fuel consumption to place the spacecraft there. The results are also shown in Table 4 for the situation where  $r_p$  is equal to 30,000 km. The interesting characteristic is that it is possible to find a sequence with more swing-bys. In this case, a number of six swing-bys, instead of four, were found. The successive values of energy (and so semi-major axis) are the same, but since the initial eccentricity is smaller, the perigee does not reach the surface of the Earth and the sequence has two more swing-bys. It means that the duration of the sequence is larger, in the order of 546 days, instead of 355 days. The maximum value of the apogee distance is 529,720.85 km, a little larger than the value of 522,784.43 km, found before, and two more intermediate steps were added. So, the decision of starting with a higher

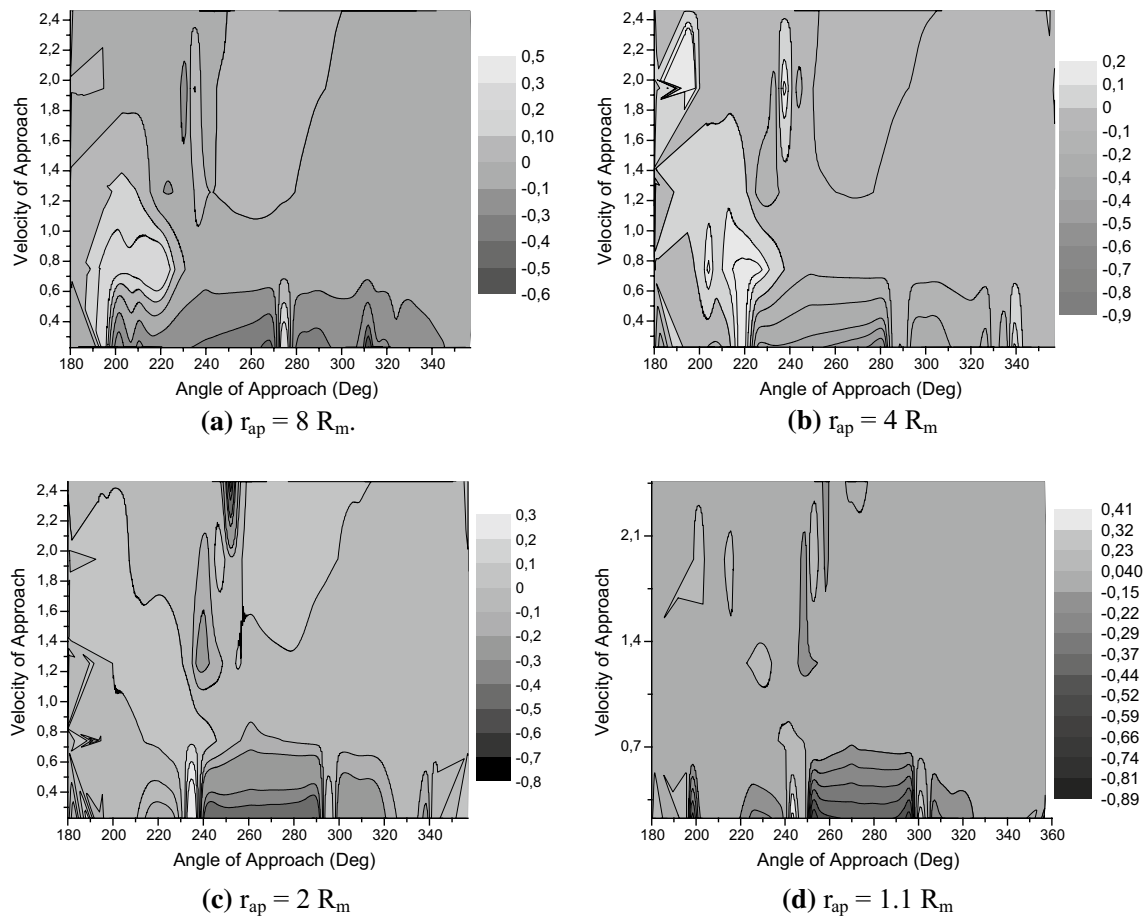


**Fig. 15** Difference of the variation in energy between two models for different values of the close approach distance

perigee depends on the goals of the mission. There is a trade-off between the fuel consumption to place the spacecraft in the initial orbit and the time and sequence of orbits obtained. The criterion of Tisserand confirms the trajectories found one more time, with the errors still in the order of the fourth decimal digit, so it is possible to be sure about the existence of the sequence of trajectories proposed.

#### 4.2 Study of the accuracy of the “patched-conics” method for the Earth–Moon system

Another interesting question that can be made now is how accurate is the “patched-conics” approach for the Earth–Moon system. A detailed study is shown in Ref. [34] for the Sun–Jupiter system but, since the Moon has a much larger mass with respect to the Earth than Jupiter has with respect to the Sun (about 10 times), this approximation is expected to give results with less accuracy. To answer this question, a study similar to the one shown in Ref. [34] is performed here for the Earth–Moon system. Simulations are made using the circular-restricted three-body problem and the “patched-conics” approach for a large number of

swing-bys and the differences are plotted in a graph that has the angle of approach in the horizontal axis (in degrees) and the velocity of approach in the vertical axis (in canonical units). Figure 15 shows the results for different values of the close approach distance.

Another view of the same results can be done by calculating the errors as a percentage. These calculations are made using:

$$Ea = \left| \frac{EP2C - EPC}{\Delta Em} \right| \times 100 \tag{26}$$

In this equation, EPC is the variation of energy calculated using the model given by the restricted three-body problem, EP2C is the same variation obtained by the “patched-conics” approach and  $\Delta Em$  is the mean variation of each graph. The mean variation is used instead of the instantaneous value of every trajectory to avoid numerical problems with low values in the denominator for regions where the variation of energy is near zero. The figures are similar to the ones shown above, so they are omitted here to save space. But, in general, it is clear that the errors are larger when compared to the Sun–Jupiter system [34], as expected. For

**Table 5** Numerical results of energy variation between two models for perigee distance of 2 radius of the Moon

*CJ* Jacobian’s constant  $V_{inf}$  velocity (canonical units)

$\psi$ (°)	Energy (canonical units)	$C_{j_i} = -1.3$	$C_{j_i} = -1.0$	$C_{j_i} = -0.7$	$C_{j_i} = -0.4$	$C_{j_i} = -0.1$	$C_{j_i} = 0.2$	$C_{j_i} = 0.5$	$C_{j_i} = 0.8$	$C_{j_i} = 1.1$	$C_{j_i} = 1.4$
		$C_{j_f} = -1.0$	$C_{j_f} = -0.7$	$C_{j_f} = -0.4$	$C_{j_f} = -0.1$	$C_{j_f} = 0.2$	$C_{j_f} = 0.5$	$C_{j_f} = 0.8$	$C_{j_f} = 1.1$	$C_{j_f} = 1.4$	$C_{j_f} = 1.7$
		$V_i = 0.59$	$V_i = 0.97$	$V_i = 1.24$	$V_i = 1.47$	$V_i = 1.66$	$V_i = 1.83$	$V_i = 1.99$	$V_i = 2.13$	$V_i = 2.27$	$V_i = 2.35$
		$V_f = 0.97$	$V_f = 1.24$	$V_f = 1.47$	$V_f = 1.66$	$V_f = 1.83$	$V_f = 1.99$	$V_f = 2.13$	$V_f = 2.27$	$V_f = 2.35$	$V_f = 2.48$
180°–190°	$ \Delta Em $	0.010	0.006	0.004	0.003	0.003	0.002	0.002	0.002	0.002	0.001
	$\Delta Em3c$	0.103	0.101	0.106	0.100	0.096	0.092	0.088	0.106	0.104	0.080
190°–200°	$ \Delta Em $	0.026	0.015	0.010	0.008	0.006	0.005	0.003	0.003	0.003	0.003
	$\Delta Em3c$	0.299	0.309	0.303	0.290	0.278	0.267	0.256	0.247	0.260	0.256
200°–210°	$ \Delta Em $	0.033	0.024	0.017	0.012	0.009	0.007	0.006	0.005	0.004	0.003
	$\Delta Em3c$	0.424	0.512	0.501	0.480	0.460	0.441	0.424	0.408	0.396	0.381
210°–220°	$ \Delta Em $	0.059	0.033	0.022	0.015	0.012	0.009	0.007	0.006	0.005	0.004
	$\Delta Em3c$	0.668	0.689	0.673	0.645	0.619	0.594	0.571	0.550	0.533	0.514
220°–230°	$ \Delta Em $	0.077	0.043	0.028	0.020	0.015	0.012	0.010	0.008	0.006	0.006
	$\Delta Em3c$	0.839	0.863	0.842	0.808	0.775	0.744	0.716	0.690	0.668	0.645
230°–240°	$ \Delta Em $	0.076	0.041	0.027	0.019	0.014	0.010	0.009	0.007	0.006	0.005
	$\Delta Em3c$	0.826	0.849	0.828	0.794	0.761	0.730	0.702	0.676	0.655	0.632
240°–250°	$ \Delta Em $	0.107	0.056	0.036	0.024	0.018	0.013	0.010	0.008	0.006	0.005
	$\Delta Em3c$	1.077	1.102	1.073	1.028	0.985	0.944	0.907	0.873	0.844	0.815
250°–260°	$ \Delta Em $	0.087	0.060	0.038	0.026	0.019	0.015	0.011	0.009	0.007	0.006
	$\Delta Em3c$	1.032	1.174	1.142	1.096	1.051	1.008	0.969	0.934	0.903	0.873
260°–270°	$ \Delta Em $	0.117	0.069	0.039	0.025	0.018	0.013	0.010	0.007	0.005	0.004
	$\Delta Em3c$	1.179	1.210	1.178	1.123	1.076	1.033	0.993	0.956	0.924	0.893
270°–280°	$ \Delta Em $	0.116	0.059	0.037	0.024	0.017	0.012	0.009	0.007	0.004	0.004
	$\Delta Em3c$	1.179	1.203	1.170	1.122	1.076	1.032	0.992	0.956	0.923	0.893
280°–290°	$ \Delta Em $	0.112	0.057	0.035	0.022	0.015	0.011	0.008	0.006	0.004	0.003
	$\Delta Em3c$	1.146	1.171	1.138	1.092	1.046	1.003	0.964	0.928	0.896	0.865
290°–300°	$ \Delta Em $	0.100	0.050	0.031	0.020	0.014	0.010	0.006	0.004	0.003	0.002
	$\Delta Em3c$	1.069	1.093	1.063	1.021	0.979	0.940	0.903	0.870	0.840	0.813
300°–310°	$ \Delta Em $	0.087	0.044	0.027	0.017	0.012	0.009	0.006	0.004	0.003	0.001
	$\Delta Em3c$	0.964	0.988	0.961	0.924	0.886	0.851	0.818	0.788	0.762	0.736
310°–320°	$ \Delta Em $	0.071	0.037	0.022	0.014	0.009	0.007	0.004	0.003	0.002	0.001
	$\Delta Em3c$	0.831	0.855	0.831	0.800	0.767	0.737	0.708	0.683	0.659	0.637
320°–330°	$ \Delta Em $	0.054	0.055	0.029	0.018	0.008	0.005	0.004	0.002	0.001	0.001
	$\Delta Em3c$	0.664	0.675	0.696	0.677	0.626	0.601	0.578	0.557	0.537	0.521
330°–340°	$ \Delta Em $	0.038	0.021	0.013	0.009	0.006	0.004	0.003	0.002	0.001	0.0004
	$\Delta Em3c$	0.491	0.509	0.494	0.477	0.457	0.438	0.421	0.405	0.390	0.3779
340°–350°	$ \Delta Em $	0.022	0.012	0.008	0.005	0.005	0.002	0.002	0.001	0.001	0
	$\Delta Em3c$	0.301	0.313	0.304	0.294	0.294	0.271	0.260	0.251	0.241	0.234
350°–360°	$ \Delta Em $	0.007	0.004	0.003	0.001	0.001	0	0.001	0.001	0	0
	$\Delta Em3c$	0.107	0.111	0.106	0.104	0.100	0.096	0.093	0.090	0.085	0.084

the study considering the case  $r_{ap} = 8 R_m$ , 305 swing-bys were obtained and the error between both models is in the range 10–80 %, from a total of 3,660 swing-bys. For the situation, where  $r_{ap} = 4 R_m$ , 127 swing-bys had errors above 10 % from a total of 3,660 swing-bys. Another value used for the close approach distance in this test was  $r_{ap} = 2 R_m$ . In this case we found 125 swing-bys with errors in the range

10–100 %, also from a total of 3,660 swing-bys calculated. As a final simulation, the case  $r_{ap} = 1.1 R_m$  was used. Here we found 102 swing-bys with errors in the range 10–100 %, also from a total of 3,660 swing-bys.

The results show that the accuracy of the method improves when the value of  $r_{ap}$  decreases and the effects of the close approaches are larger. In the region where practical

applications are more numerous,  $r_{ap} < 4.0 R_m$ , there are only around 120 swing-bys (about 3 % of the total) that have more than 10 % in error. It makes this method of evaluation of the accuracy useful for preliminary analyses of the problem. Another point in favor of this analysis is that the regions where the accuracy is not good (>10 %) are shown and, if the trajectory of interest lies in this region, a better method can be used to evaluate the results of the swing-bys, as the restricted three-body problem.

Another view with more details of the comparison of the models, “patched conics” and “Restricted Three-Body Problem”, is shown in Table 5. In this study, 450,000 maneuvers were performed for the periapsis distance of 2 radius of the Moon. In all cases studied was analyzed energy change when considering different angle of approaches and different Jacobi’s constant. The results are organized in Table 5, where  $|Geml| = |\Delta Em_{PC} - \Delta Em_{3c}|$ ;  $\Delta Em_{3c}$  calculated using the model given by the restricted three-body problem.  $\Delta Em_{PC}$  is the same variation obtained by the “patched-conics” approach and  $\Delta Em$  is the mean variation between two models for each simulation;  $c_{j_i}$  and  $c_{j_f}$  are the Jacobi’s constants initial and final, respectively;  $v_i$  and  $v_f$  is the initial and final velocity in the canonical units which corresponds to  $c_{j_i}$  and  $c_{j_f}$ .

## 5 Conclusion

This study was made to show the evolution of the trajectories, as well as the amplitudes of the variations of the velocity, energy and angular momentum of an orbit due to a series of close approaches with the Moon. A set of analytical equations is derived to allow the calculation of the distance of the closest approach that generates a specified orbit. Then, a series of resonant orbits with the Moon that has increasing apoapsis to cover a large area of the space around the Earth–Moon system is found. Using these equations it is possible to establish a sequence of close approaches that meets the goals.

The results showed that it is possible to find useful sequences of close approaches using these natural changes of orbits to pass by different positions in the space without the expenses of applying a control to the spacecraft. The criterion of Tisserand was applied and it confirmed the existence of the trajectories found.

Regarding the study of the accuracy of the “patched-conics” method used to study this problem, it was shown that its accuracy improves when the distance of the close approach decreases, which is very important because the practical applications concentrated in this region. In general, it is clear that the approximation is good in the majority of the initial conditions. The situations where the accuracy is not so good are mapped, so it is possible to know in advance that a better solution has to be found.

**Acknowledgments** The authors wish to express their appreciation for the support provided by Grants # 473387/2012-3 and 304700/2009-6, from the National Council for Scientific and Technological Development (CNPq); grants # 2011/08171-3, 2011/13101-4, 2014/06688-7 and 2012/21023-6, from São Paulo Research Foundation (FAPESP) and the financial support from the National Council for the Improvement of Higher Education (CAPES).

## References

- Allen JAV (2003) Gravitational assist in celestial mechanics—a tutorial. *Am J Phys* 71:448–4515
- Battin RH (1987) An introduction to the mathematics and models of astrodynamics. AIAA, New York
- Broucke RA (1988) The Celestial mechanics of gravity assist. In: AIAA/AAS Astro Conf Minneapolis. AIAA paper 88-4220, August
- Casalino L, Colasurdo G, Pasttrone D (1999) Optimal low-thrust escape trajectories using gravity assist. *J Guid Control Dyn* 22(5):637–642
- D’Amario LA, Byrnes DV, Stanford RH (1982) Interplanetary trajectory optimization with application to Galileo. *J Guid Control Dyn* 5(5):465–471
- Dowling RL, Kosmann WJ, Minovitch MA, Ridenoure RW (1991) Gravity propulsion research at UCLA and JPL. In: 41st Con of the IAF Dresden GDR Oct 1962–1964
- Ederly A, Schiff C (2001) The double lunar swing-by of the MMS mission. In: 16th international symposium on space flight dynamics, Pasadena CA
- Farquhar R, Muhonen D, Church LC (1985) Trajectories and orbital maneuvers for the ISEE-3/ICE comet mission. *J Astronaut Sci* 33(3):235–254
- Farquhar RW, Dunham DW (1981) A new trajectory concept for exploring the Earth’s geomagnetic tail. *J Guid Control Dyn* 4(2):192–196
- Flandro G (1966) Fast reconnaissance missions to the outer Solar System utilizing energy derived from the gravitational field of Jupiter. *Astronaut Acta* 12(4):329–337
- Formiga JKS, Prado AFBA (2014) An analytical description of the three-dimensional swing-by. *Comp Appl Math* 1:3–18
- Formiga JKS, Prado AFBA (2013) Searching sequences of resonant orbits between a spacecraft and Jupiter. *J Phys: Conf Ser* 465:1–6
- Gobet FW, Doll JR (1969) A survey of impulsive trajectories. *AIAA J* 7:801–834
- Gomes VM, Prado AFBA (2012) Low-thrust out-of-plane orbital station-keeping maneuvers for satellites. *Math Prob Eng (Print)*, 1–14
- Gross LR, Prussing JE (1974) Optimal multiple-impulse direct ascent fixed-time rendezvous. *AIAA J* 12(7):885–889
- Hoelker RF, Silber R (1959) The bi-elliptic transfer between circular co-planar orbits. Tech Memo, Army Ballistic Missile Agency, Redstone Arsenal, Alabama, USA, pp 2–59
- Hohmann W (1925) Die Erreichbarkeit der Himmelskörper. Oldenbourg, Munich (in German)
- Kizner W (1961) A Method of describing miss distances for lunar and interplanetary trajectories. *Planet Space Sci* 7:125
- Marchal C (1965) Transferts optimaux entre orbites elliptiques coplanaires (Durée indifférente). *Astrol Acta* 11(6):432–445 (in French)
- Lawden DF (1953) Minimal rocket trajectories. *ARS J* 23(6):360–382
- Lawden DF (1954) Fundamentals of space navigation. *JBIS* 13:87–101

22. Marec JP (1979) Optimal space trajectories. Elsevier, New York
23. Marsh SM, Howell KC (1988) Double lunar swing by trajectory design. AIAA paper 88–4289
24. Miller JK, Weeks CJ (2002) Application of tisserand's criterion to the design of gravity assist trajectory. AIAA paper 2002–4717
25. Strange NJ, Longuski JM (2002) Graphical method for gravity-assist trajectory design. *J Space Roc* 39(1):9–16
26. Petropoulos AE, Longuski JM, Vinh NX (1999) Shape-based analytic representations of low-thrust trajectories for gravity-assist applications. Amer Ast Soc, AAS Paper 99–337, August
27. Petropoulos A E, Longuski JM (2000) Automated design of low-thrust gravity-assist trajectories. AIAA paper 2000–4033, august
28. Prado AFBA, Broucke RA (1995) Transfer orbits in restricted problem. *J Guid Control Dyn* 18(3):593–598
29. Prado AFBA, Broucke RA (1995) Effects of atmospheric drag in swing-by trajectory. *Acta Astrol* 36(6):285–290
30. Prado AFBA, Broucke RA (1996) Transfer orbits in the Earth-Moon system using a regularized model. *J Guid Control Dyn* 19(4):929–933
31. Prado AFBA (1996) Traveling between the lagrangian points and the Earth. *Acta Astrol* 39(7):483–486
32. Prado AFBA (1997) Powered swing-by. *J Guid Control Dyn* 19(5):1142–1147
33. Prado AFBA (1997) Close-approach trajectories in the elliptic restricted problem. *J Guid Control Dyn* 20(4):797–802
34. Prado AFBA (2007) A comparison of the patched-conics approach and the restricted problem for swing-bys. *Adv Space Res* 40:113–117
35. Prussing JE, Chiu JH (1986) Optimal multiple-impulse time-fixed rendezvous between circular orbits. *J Guid Control Dyn* 9(1):17–22
36. Prussing JE (1969) Optimal four-impulse fixed-time rendezvous in the vicinity of a circular orbit. *AIAA J* 7(5):928–935
37. Prussing JE (1970) Optimal two- and three-impulse fixed-time rendezvous in the vicinity of a circular orbit. *AIAA J* 8(7):1221–1228
38. Shternfeld A(1959) Soviet space science, Basic Books, Inc., New York, 109–111
39. Striepe SA, Braun RD (1991) Effects of a Venus swing by periapsis burn during an Earth-Mars trajectory. *J Astrol Sci* 39(3):299–312
40. Sukhanov AA, Prado AFBA (2001) Constant tangential low-thrust trajectories near an oblate planet. *J Guid Control Dyn* 24(4):723–731
41. Swenson BL (1992) Neptune atmospheric probe mission. In: AIAA7AAS Astr. Conf., Hilton Head, SC, AIAA paper 92–4371
42. Szebehely V(1967) Theory of orbits: the Restricted Problem of Three Bodies, Academic Press, New York, 67, 586–587
43. Weinstein SS(1992) Pluto flyby mission design concepts for very small and moderate spacecraft. AIAA paper 92–4372. In: AIAA/AAS Astr. Conf. Hilton Head, SC, Aug. 10–12
44. Miller JK, Weekst CJ (2002) Application of Tisserand's criterion to the design of gravity assist trajectories. AIAA paper 2002–4717